

Carrier density dependence of mobility in organic solids: A Monte Carlo simulation

J. Zhou,¹ Y. C. Zhou,¹ J. M. Zhao,¹ C. Q. Wu,² X. M. Ding,¹ and X. Y. Hou^{1,*}

¹*Surface Physics Laboratory (National Key Laboratory), Fudan University, Shanghai 200433, China*

²*Department of Physics, Fudan University, Shanghai 200433, China*

(Received 15 February 2007; published 2 April 2007)

The multicarrier hopping process in disordered organic materials is studied via Monte Carlo simulations taking into consideration both the site exclusion effect and Coulomb interaction. The carrier mobility in materials with Gaussian energetic disorder is found to depend heavily on carrier density. At high carrier densities, the Coulomb interaction is found to reduce the carrier mobility in materials with low intrinsic disorder or at high temperatures, and to enhance the mobility in materials with high intrinsic disorder or at low temperatures.

DOI: [10.1103/PhysRevB.75.153201](https://doi.org/10.1103/PhysRevB.75.153201)

PACS number(s): 72.20.Ee, 72.80.Le, 72.80.Ng

Recently, interest in organic field-effect transistors (OFETs) is growing rapidly as their mobilities are approaching those in amorphous-silicon transistors.^{1,2} One of the unique properties found in OFETs is the superlinear increase in mobility with carrier density.³ This increase has been explained based on the following two considerations: (i) carriers transport via hopping among localized states (or transport sites) such as molecules or polymer chain segments in organic solids; (ii) two carriers cannot occupy one single transport site, which is referred to as the site exclusion effect (SEE) hereafter. Qualitatively, the mobility increase has been attributed to the gradual filling of lower-energy transport sites as the carrier density increases and, consequently, the decrease of the activation energy carriers need for hopping to neighboring sites.⁴ Quantitatively, several analytical works have studied the effect of the partial filling of density of states (DOS) on charge transport and have found the mobility increase with carrier density,^{5–11} as reviewed by Coehoorn *et al.*¹² More recently, Pasveer *et al.*¹³ have studied the mobility dependence on carrier density by numerically solving the master equation describing multiple-carrier hopping.

All of those works have considered the SEE by adopting Fermi-Dirac statistics; however, none has considered the Coulomb interaction between charge carriers. In organic materials, the Coulomb interaction would have a profound effect on charge transport and should not be neglected for the following reasons: (i) charge carriers are strongly localized and should be regarded as point charges; (ii) dielectric constants are small (typically 3–5) so that the effective range of Coulomb interaction is long; and (iii) near the semiconductor-insulator interface in OFETs, carrier densities can exceed 10^{19} cm^{-3} (Ref. 3) so that the average distance between carriers is short. Since the random hopping of carriers induces random Coulomb interactions, it is difficult to describe them analytically or with a master equation. However, Monte Carlo (MC) simulation has a special advantage in treating the interactions straightforwardly.

Previously, MC simulations assuming both the energetic and the positional disorder in Gaussian distribution have successfully explained the carrier transport in organic materials at low carrier densities.^{14–16} Unfortunately, these MC simulations involve only a single carrier in each run, making them invalid for systems at high carrier densities with both the SEE and Coulomb interaction. Recently, Houili *et al.* per-

formed a three-dimensional (3D) multiparticle MC simulation to study the charge transport across the heterojunction between layers of different organic materials and found that the Coulomb interaction assists charge carriers to overcome the transport barrier at the interface.¹⁷ However, they focused only on the interfacial properties of organic light-emitting diodes with relatively low average carrier densities, rather than the bulk properties of carrier transport at high carrier densities typically observed in OFETs.

In this Brief Report, a MC method taking into consideration both the SEE and the Coulomb interaction is devised to study the multiple-carrier hopping in disordered organic materials and the dependence of mobility on carrier density. The effect of Coulomb interaction on the charge transport at high carrier densities is also explored by comparing the results with or without the Coulomb interaction.

For comparison with most previous works in the literature, we assume the Gaussian disorder model,¹⁴ in which the hopping rate of carriers is governed by the Miller-Abrahams equation,¹⁸

$$v_{ij} = \begin{cases} v_0 \exp(-\Gamma r_{ij}) \exp[-(\epsilon_j - \epsilon_i)/kT], & \epsilon_j > \epsilon_i \\ v_0 \exp(-\Gamma r_{ij}), & \epsilon_j \leq \epsilon_i, \end{cases} \quad (1)$$

where v_{ij} is the jump rate from site i to site j , v_0 the intrinsic attempt frequency, Γ the coefficient of intersite coupling, r_{ij} the intersite distance between i and j , and ϵ the site energy.

We use 3D cubic lattices of lattice constant a and with 3D periodic boundary condition (PBC) to simulate the bulk properties of carrier transport in organic materials. Each lattice point represents a transport site; the entire lattice contains $L \times L \times L$ sites (in the present work, we take $L=51$ which is large enough to avoid the finite-size effect). We consider N carriers together in each simulation run, so that the site occupation ratio $\rho=N/L^3$. The energy of each transport site is randomly drawn from a Gaussian distribution $(2\pi\sigma^2)^{-1/2} \exp(-\epsilon^2/2\sigma^2)$, where σ denotes the magnitude of energetic disorder. The positional disorder is neglected for simplicity in the present work and will be studied elsewhere. We also limit the carrier hops to occur only between the nearest-neighboring sites, which is valid in the range of σ/kT used in the present work.¹²

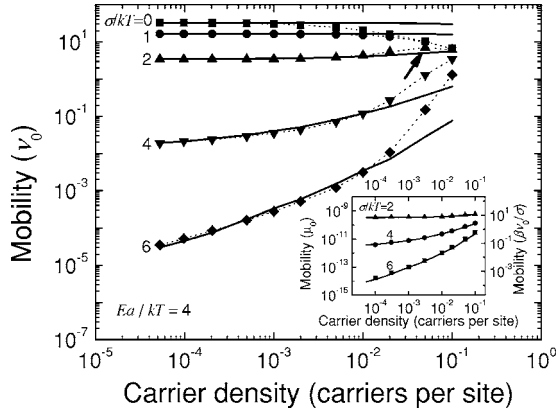


FIG. 1. Calculated carrier density dependence of mobility for various values of σ/kT with (data points) and without (solid curves) the Coulomb interaction. The dotted lines are guides for the eye. The arrow indicates a transition from CIIMB to CIIMD. Inset: Comparison between present results without the Coulomb interaction (solid curves, right y axis, in the unit of $\beta\nu_0/\sigma$) and those reported in Ref. 13 (data points, left y axis, in the unit of μ_0). Note that μ_0 is defined by Eq. (3c) in Ref. 13 and is related to σ . Our results are based on ν_0 so a conversion is needed. β is an arbitrary constant.

After carriers are introduced into the lattice, the energy of any transport site will be shifted by the Coulomb potentials of these carriers as well as their periodic images due to the long-range nature of the Coulomb interaction. Although such Coulomb potentials in simulations with 3D PBC are usually treated with the Ewald method,¹⁹ we find it also possible to tackle the present problem of carrier hopping by directly calculating the difference in Coulomb potential $\Delta\phi(t,s)$ between the source (s) and target (t) sites of a given hop,

$$\begin{aligned} \Delta\phi(t,s) &= \sum'_i \Delta\phi_i(t,s) \\ &= \frac{e^2}{4\pi\epsilon_0\epsilon_r} \sum'_i \sum_{\mathbf{n}} \left(\frac{1}{|\mathbf{r}_i + \mathbf{n} - \mathbf{r}_t|} - \frac{1}{|\mathbf{r}_i + \mathbf{n} - \mathbf{r}_s|} \right), \end{aligned} \quad (2)$$

where $\Delta\phi_i(t,s)$ is the contribution to $\Delta\phi(t,s)$ from the i th carrier, \mathbf{r}_s , \mathbf{r}_t , and \mathbf{r}_i are the positions of the hopping source site, target site, and the i th carrier, respectively, and $\mathbf{r}_i + \mathbf{n}$ ($\mathbf{n} = n_x\mathbf{L}_x + n_y\mathbf{L}_y + n_z\mathbf{L}_z$, $n_x, n_y, n_z \in \mathbf{Z}$, $\mathbf{n} \neq 0$) are the positions of the periodic images of the i th carrier. Note the prime on the summation over i in Eq. (2) denotes that the calculated $\Delta\phi(t,s)$ is the sum of the contributions from all carriers except the hopping one, since the hopping carrier does not exert any Coulomb force on itself. The direct calculation of $\Delta\phi(t,s)$ via Eq. (2) converges fast enough if s and t are neighboring sites. We adopt a universal dielectric constant of 4.0 in all simulations, a value commonly found in organic materials.

A typical simulation runs as follows.

(1) A certain number of carriers are first put on different sites randomly.

(2) The hopping rates $\nu_{n\alpha}$ for every carrier to hop to any of its six nearest-neighboring sites are calculated according to Eq. (1) and treated as the “hopping candidates” for the next hop, where n and α denote the index of the carrier and the index of its neighboring sites, respectively. The energy difference $\epsilon_j - \epsilon_i$ consists of three contributions: (i) the site energy difference originating from the intrinsic material disorder imposed by the Gaussian DOS, (ii) the potential difference caused by the externally applied electric field E , and (iii) the Coulomb potential difference $\Delta\phi(t,s)$. If the β th neighboring site of the m th carrier is currently occupied by another carrier, $\nu_{m\beta}$ is set to be zero, as required by the SEE. To examine the effect of Coulomb interaction on carrier mobility, we also conducted simulations without Coulomb interactions by calculating $\epsilon_j - \epsilon_i$ with just the first two contributions described above.

(3) The waiting time for the next hop τ , the index of the next carrier to hop m , and the index of the neighboring target site κ are determined by the following equations:

$$\nu_{\text{tot}} = \sum_{n\alpha} \nu_{n\alpha}, \quad \tau = -\ln(\xi_1)/\nu_{\text{tot}},$$

$$\left(\sum_{n=1}^{m-1} \sum_{\alpha=1}^6 \nu_{n\alpha} + \sum_{\alpha=1}^{\kappa-1} \nu_{m\alpha} \right) < \xi_2 \nu_{\text{tot}} < \left(\sum_{n=1}^{m-1} \sum_{\alpha=1}^6 \nu_{n\alpha} + \sum_{\alpha=1}^{\kappa} \nu_{m\alpha} \right), \quad (3)$$

where $1 \leq m \leq N$, $1 \leq \kappa \leq 6$, ν_{tot} is the total hopping rate, and ξ_1 and ξ_2 are both random numbers uniformly distributed between 0 and 1.

(4) The simulation run restarts from step (2) and continues the above steps.

The simulation is first run for enough time to get the carriers relaxed in energy. Then, we start to record the time and the hopping direction of every hop and derive the carrier mobility as

$$\mu = \frac{(l_1 - l_2)a}{NEt}, \quad t = \sum_k \tau_k, \quad (4)$$

where l_1 and l_2 are the total number of hops of all carriers along and opposite to the field direction within the recorded time t , respectively. The simulation run ends when the derived mobility converges to a certain value. The simulation with the same set of parameters is conducted for 10–50 different runs to reduce the variation of the resulting mobility value.

Figure 1 shows the carrier density dependence of mobility both with and without the Coulomb interaction for materials with various energetic disorders σ and under different temperatures T , both factors included in the dimensionless parameter σ/kT . The present MC results without the Coulomb interaction, fitting well with those from solving the master equation in Ref. 13 as shown in the inset of Fig. 1, show a superlinear increase in mobility with carrier density. The MC simulations with the Coulomb interaction lead mostly to the same mobility dependence on carrier density as simulations without the Coulomb interaction at moderate carrier densities. However, two unique features of mobility, not found in

TABLE I. Average height of energy barriers against the hopping candidates upward in energy for simulation systems characterized by σ/kT . The carrier density is 0.1 per site and the electric field is zero.

σ/kT	Barrier height without Coulomb interaction (kT)	Barrier height with Coulomb interaction (kT)
0	0.00	2.80
1	1.47	3.05
4	7.40	6.72
6	11.3	10.3

previous studies without considering the Coulomb interaction, begin to emerge as carrier density exceeds 0.01 per site. One is the drop in mobility by orders of magnitude with increasing carrier density for small σ/kT [referred to as Coulomb-interaction-induced mobility drop (CIIMD), hereafter]; the other is the even stronger increase in mobility with carrier density than the increase without the Coulomb interaction for large σ/kT [referred to as Coulomb-interaction-induced mobility boost (CIIMB), hereafter].

We took snapshots of the simulation systems both with and without the Coulomb interaction at zero electric field every 10^5 hops and listed in Table I the calculated average barrier heights of the hopping candidates upward in energy, which are the bottleneck of hopping transport. The average hopping barrier for the material with zero intrinsic disorder at a carrier density of 0.1 per site increases from 0 to $2.80kT$ upon the introduction of Coulomb interaction. A similar increase in the barrier height is also observed for $\sigma/kT=1$. Such an increase means carriers have to hop over higher barriers, resulting in the mobility drop, i.e., the CIIMD. To view how the barrier heights increase, we draw energy diagrams of the transport sites. In the extreme case where $\sigma/kT=0$, all sites have the same intrinsic energy. If there is no Coulomb interaction between carriers, the only source of the site energy difference is the applied potential. Therefore, the energy landscape of transport sites is smooth, as shown in the left half of Fig. 2(a), and carriers can easily hop without overcoming any barrier. However, if the Coulomb interaction exists, the energy of every site is shifted by the Coulomb potentials of the carriers at other sites. Due to the stochastic nature of hopping, carriers are randomly distributed in space and the shifts in site energy are also random. As shown in the right half of Fig. 2(a), such shifts result in the increase of the average hopping barrier, as well as a rough and random site-energy landscape, equivalent to some energetic disorder. Therefore, we attribute the CIIMD to extra energetic disorder induced by the Coulomb interaction. For materials with nonzero intrinsic energetic disorder, the combination of the intrinsic disorder and the Coulomb-interaction-induced disorder is complex and it is expected that a higher intrinsic disorder will screen a lower Coulomb-interaction-induced disorder and vice versa; therefore, the CIIMD gradually disappears as σ/kT increases (from 0 to 2 for the parameters in our simulation).

In cases where σ/kT are large, most carriers occupy low-energy sites and the hopping barriers are usually high. Thus,

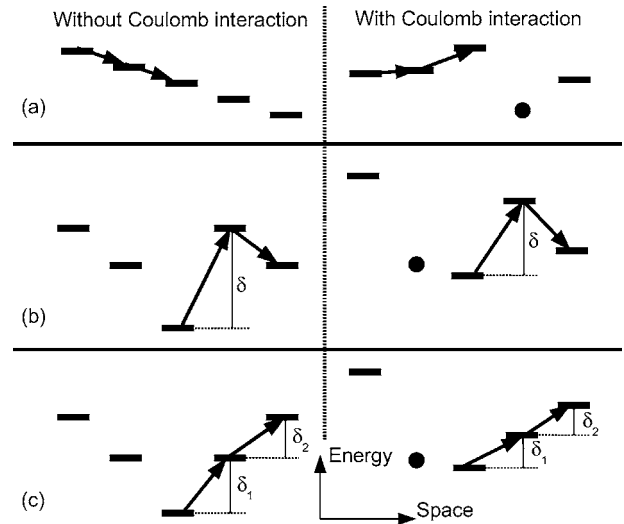


FIG. 2. Energy diagrams of transport sites. The energy and position of a transport site is denoted by a horizontal line. In each subfigure, the left and right halves depict the cases without and with the Coulomb interaction, respectively. Arrows denote the route of a hopping carrier (not explicitly plotted). The energies of transport sites are in reference to the hopping carrier and are shifted by an additional carrier explicitly plotted as a dot. (a) The energy diagram for $\sigma/kT=0$ under an applied field. [(b) and (c)] Energy diagrams for two examples of high σ/kT under zero field, showing how the hopping barriers δ are reduced by the Coulomb interaction.

the mobility in high-disorder materials is usually low at moderate carrier densities. In previous works, the mobility increase with carrier density by orders of magnitude has been solely attributed to the SEE.⁴ We find that the Coulomb interaction also plays a role in increasing the mobility at high carrier densities, i.e., the CIIMB. From the snapshots of simulation systems with large σ/kT as described in the previous paragraph, we find that the average hopping barrier for $\sigma/kT=6$ at a carrier density of 0.1 per site has dropped from $11.3kT$ to $10.3kT$ upon the introduction of the Coulomb interaction. A similar drop in hopping barrier is also found for $\sigma/kT=4$. Such a drop facilitates carrier hopping and leads to the CIIMB. Since low-energy sites are the limiting factor for carrier transport in cases of large σ/kT , we focus our attention on these sites and plot the energy diagrams of transport sites near a low-energy site. For either of the two examples shown in Figs. 2(b) and 2(c), the energy barrier keeping the carrier at the low-energy site from hopping away is reduced by the Coulomb potential of another carrier at a neighboring site. Thus, the carrier at the low-energy site can hop away more easily and that site would be less likely to trap either carrier.

It is necessary to understand the link between the apparently opposite roles the Coulomb interaction plays at high carrier densities for different σ/kT . When σ/kT is small, the extra disorder is important as it cannot be completely screened out by the intrinsic disorder of material; the number of low-energy sites is small so that the effect of the Coulomb interaction on reducing hopping barriers is also quite limited. Therefore, only the CIIMD would be observed. However, when σ/kT is large, the Coulomb-interaction-induced extra

disorder is totally screened by the intrinsic disorder; the large number of low-energy sites makes it significant that the hopping barrier is reduced by the Coulomb interaction. Therefore, only the CIIMB would be observed. For materials with moderate σ/kT , e.g., $\sigma/kT=2$, a transition between the CIIMD and CIIMB could be observed, as indicated by an arrow in Fig. 1. Furthermore, the combination of the CIIMD and CIIMB remarkably reduces the difference in mobility between systems of different σ/kT at carrier densities as high as 10^{-1} carriers per site, compared with the difference without considering the Coulomb interaction.

It should be noted that in real OFETs, a large amount of carriers opposite in polarity to those in the organic layer exist at the gate-insulator interface, and the distribution of carriers in the organic layer perpendicular to the channel is not uniform.²⁰ These factors are not included in the present simulation because we focus on the microscopic charge hopping process in the organic materials to derive the relations between the bulk carrier mobility and carrier density. The charges of opposite polarity at the gate-insulator interface only form a uniform electric field in the organic layer, and therefore are not expected to change the transport property.

After knowing the bulk mobility for any set of parameters such as electric field, temperature, material disorder, and carrier density, one can further derive the performances of a real OFET by solving equations considering the spatial distribution of carrier density and electric field, as well as real device parameters.

In conclusion, we have demonstrated MC simulations of the carrier density dependence of mobility in disordered organic materials, taking into account both the SEE and the Coulomb interaction between carriers. It is found that when the carrier density exceeds 10^{-2} carriers per site: (i) in cases of low σ/kT , Coulomb interaction induces extra energetic disorder in the system and reduces the carrier mobility with increasing carrier density; (ii) in cases of high σ/kT , Coulomb interaction reduces the energy barriers against carrier hopping and causes a steeper increase of mobility with carrier density than that caused by the SEE only.

This work is supported by the CNKBRFSF and the National Natural Science Foundation of China under Grant No. 10321003.

*Electronic address: xyhou@fudan.edu.cn

¹H. Siringhaus, *Adv. Mater. (Weinheim, Ger.)* **17**, 2411 (2005).
²L. L. Chua, J. Zaumseil, J. F. Chang, E. C. Ou, P. K. Ho, H. Siringhaus, and R. H. Friend, *Nature (London)* **434**, 194 (2005).
³C. Tanase, E. J. Meijer, P. W. M. Blom, and D. M. de Leeuw, *Phys. Rev. Lett.* **91**, 216601 (2003).
⁴C. Tanase, P. W. M. Blom, D. M. de Leeuw, and E. J. Meijer, *Phys. Status Solidi A* **201**, 1236 (2004).
⁵V. I. Arkhipov, P. Heremans, E. V. Emelianova, G. J. Adriaenssens, and H. Bässler, *J. Phys.: Condens. Matter* **14**, 9899 (2002).
⁶M. C. J. M. Vissenberg and M. Matters, *Phys. Rev. B* **57**, 12964 (1998).
⁷S. D. Baranovskii, I. P. Zvyagin, H. Cordes, S. Yamasaki, and P. Thomas, *Phys. Status Solidi B* **230**, 281 (2002).
⁸S. D. Baranovskii, I. P. Zvyagin, H. Cordes, S. Yamasaki, and P. Thomas, *J. Non-Cryst. Solids* **299**, 416 (2002).
⁹R. Schmechel, *Phys. Rev. B* **66**, 235206 (2002).
¹⁰H. C. F. Martens, I. N. Hulea, I. Romijn, H. B. Brom, W. F. Pasveer, and M. A. J. Michels, *Phys. Rev. B* **67**, 121203(R)

(2003).
¹¹Y. Roichman, Y. Preezant, and N. Tessler, *Phys. Status Solidi A* **201**, 1246 (2004).
¹²R. Coehoorn, W. F. Pasveer, P. A. Bobbert, and M. A. J. Michels, *Phys. Rev. B* **72**, 155206 (2005).
¹³W. F. Pasveer, J. Cottaar, C. Tanase, R. Coehoorn, P. A. Bobbert, P. W. M. Blom, D. M. de Leeuw, and M. A. J. Michels, *Phys. Rev. Lett.* **94**, 206601 (2005).
¹⁴H. Bässler, *Phys. Status Solidi B* **175**, 15 (1993).
¹⁵Y. N. Gartstein and E. M. Conwell, *Chem. Phys. Lett.* **245**, 351 (1995).
¹⁶S. V. Novikov, D. H. Dunlap, V. M. Kenkre, P. E. Parris, and A. V. Vannikov, *Phys. Rev. Lett.* **81**, 4472 (1998).
¹⁷H. Houili, E. Tutiš, I. Batistić, and L. Zuppiroli, *J. Appl. Phys.* **100**, 033702 (2006).
¹⁸A. Miller and E. Abraham, *Phys. Rev.* **120**, 745 (1960).
¹⁹S. W. DeLeeuw, J. W. Perram, and E. R. Smith, *Proc. R. Soc. London, Ser. A* **373**, 27 (1980).
²⁰C. Tanase, E. J. Meijer, P. W. M. Blom, and D. M. de Leeuw, *Org. Electron.* **4**, 33 (2003).